HHS Public Access

Author manuscript

Mult Scler. Author manuscript; available in PMC 2022 November 01.

Published in final edited form as:

Mult Scler. 2022 November ; 28(13): 2020–2026. doi:10.1177/13524585221106290.

Mitochondrial measures in neuronally-enriched extracellular vesicles predict brain and retinal atrophy in multiple sclerosis

Dimitrios C. Ladakis, MD[1,*], **Pamela J. Yao, PhD**[2,*], **Michael Vreones, BS**[2], **Joseph Blommer, BS**[2], **Grigorios Kalaitzidis, MD**[1], **Elias S. Sotirchos, MD**[1], **Kathryn C. Fitzgerald, ScD**[1], **Shiv Saidha, MBBCh**[1], **Peter A. Calabresi, MD**[1], **Dimitrios Kapogiannis, MD**[1,2,†], **Pavan Bhargava, MD**[1,†]

[1]Department of Neurology, Johns Hopkins University School of Medicine, Baltimore, MD;

[2]Laboratory of Clinical Investigation, National Institutes of Aging, Baltimore, MD, USA

Abstract

Background: Mitochondrial dysfunction plays an important role in MS disease progression. Plasma extracellular vesicles (EVs) are a potential source of novel biomarkers in MS and some of these are derived from mitochondria and contain functional mitochondrial components.

Objective: To evaluate the relationship between levels of mitochondrial complex IV and V activity in neuronally-enriched EVs (NEVs) and brain and retinal atrophy as assessed using serial magnetic resonance imaging (MRI) and optical coherence tomography (OCT).

Methods: Our cohort consisted of 48 people with MS. NEVs were immunocaptured from plasma and mitochondrial complex IV and V activity levels were measured. Subjects underwent OCT every 6 months and brain MRI annually. The associations between baseline mitochondrial complex IV and V activities and brain substructure and retinal thickness changes were estimated utilizing linear mixed-effects models.

Results: We found that higher mitochondrial complex IV activity and lower mitochondrial complex V activity levels were significantly associated with faster whole brain volume (WBV) atrophy. Similar results were found with other brain substructures and retinal layer atrophy.

Conclusions: Our results suggest that mitochondrial measures in circulating NEVs could serve as potential biomarkers of disease progression and provide the rationale for larger follow-up longitudinal studies.

Keywords

Extracellular vesicles; mitochondrial complexes; multiple sclerosis; biomarkers

Corresponding Authors: Dimitrios Kapogiannis, MD, Address: 251 Bayview Blvd, Baltimore, MD, 21224, kapogiannisd@mail.nih.gov, Pavan Bhargava, MD, Address: 600 N Wolfe St, Pathology 627, Baltimore, MD 21287. pbharga2@jhmi.edu.

*These authors contributed equally to this work

†Senior Authors

INTRODUCTION

Mitochondrial dysfunction has been observed in MS in both lesional and non-lesional areas. In acute lesions, the activity of several mitochondrial components is reduced,[1] while, in chronically demyelinated axons, an increase in mitochondrial complex IV activity has been described.[2,3] Neuronal mitochondrial dysfunction is thought to be an important factor in disease progression, with a recent study demonstrating that, in experimental autoimmune encephalomyelitis, increasing mitochondrial function leads to neuroprotection even in the setting of neuroinflammation.[4] Furthermore, it has been shown that there is increased axonal transportation of mitochondria to active lesions as a compensation for the increased energetic demand of demyelinated axons. Enhancement of this process can lead to increased functionality of these neurons and remyelination.[5]

Recent studies have also identified the presence of protrusions in neuronal mitochondria that leads to the release of intracellular vesicles from the mitochondria that have been dubbed “mitovesicles”.[6,7] In addition, circulating Extracellular Vesicles (EVs) carry various mitochondrial cargoes (RNAs,[8] proteins), including functional mitochondrial components that may provide insight into mitochondrial function in Alzheimer’s disease (AD)[9] and other brain diseases.[10] Since we have previously identified that EVs enriched for a neuronal origin (NEVs) can identify novel biomarkers in MS,[11] we examined the activity of mitochondrial components in NEVs from people with MS (PwMS) and evaluated the ability of these measures to predict disease progression based on imaging outcomes.

METHODS

Standard Protocol Approvals, Registrations, and Patient Consents

The study protocol was approved by the Johns Hopkins Institutional Review Board and written informed consent was obtained from all study participants.

Study Cohort

We identified 48 PwMS from the Johns Hopkins MS Center. MS diagnosis was confirmed by the treating neurologist based on the 2017 revised McDonald Criteria. MS disease subtype was classified as Relapsing-Remitting, Primary Progressive or Secondary Progressive. Demographic and clinical characteristics was collected for all study subjects, including history of past optic neuritis (ON) episodes with recording of the eye and the date of the episode. Participants underwent optical coherence tomography (OCT) every 6 months and brain magnetic resonance imaging (MRI) annually. Disease modifying therapy (DMT) was updated throughout the whole follow-up period. Eyes that developed acute ON during the study (n = 2) started OCT follow-up one year following the episode.

Blood Draw

All participants had a blood draw at baseline. Approximately 10 mL of venous blood were obtained in plasma separator tubes containing ethylenediamine tetra acetic acid, incubated for 10 minutes at room temperature and then centrifuged at 3000 rpm for 15 minutes. Supernatant plasma was divided into 1.0 mL aliquots and stored at −80°C as previously

described.[12] Samples were not thawed until NEV isolation was performed. Pre-analytical factors for blood collection and storage comply with guidelines for EV biomarkers.

MRI

Brain MRI scans were performed on a 3T Philips Achieva scanner (Philips Medical System, Best, Netherlands) using three axial whole-brain sequences without gaps were utilized: multi-slice fluid-attenuated inversion recovery (FLAIR; acquired resolution: 0.8 mm × 0.8 mm × 2.2 mm; echo time (TE): 68 ms; repetition time (TR): 11 s; inversion time (TI): 2.8 s; SENSE factor: 2; averages: 1); T2-weighted dual-echo turbo spin echo (DE-TSE; acquired resolution: 0.8 mm × 0.8 mm × 2.2 mm; TE: 80 ms; TR: 4170 ms; SENSE factor: 2; averages: 1); and three-dimensional (3D) magnetization prepared rapid acquisition of gradient echoes (MPRAGE; acquired resolution: 0.8 mm × 0.8 mm × 1.2 mm; TE: 6 ms; TR: 10 ms; TI: 835 ms; flip angle: 8°; SENSE factor: 2; averages: 1).

Harmonization of the MRI images was performed using DeepHarmony.[13] Brain substructure volumes were generated by utilizing a previously described segmentation algorithm.[14] Segmentations were manually reviewed and scans with segmentation errors/failures were excluded. Statistical harmonization, via longitudinal ComBat, was applied to minimize heterogeneity related to scanner upgrades.[15]

All volumes were normalized to the intracranial volume of the corresponding participant, to account for the inter-person skull size variability. For bilateral structures, the volume fractions of right and left side were summed to calculate a total volume fraction, which was used for the analysis. Cortical gray matter (GM), subcortical GM and whole brain volume (WBV) fractions were calculated by summing the volume fractions of their components.

OCT

Retinal imaging was performed with spectral domain OCT (Cirrus HD-OCT, Model 5000, software version 11.5; Carl Zeiss Meditec, Dublin, CA), as previously described.[16] In brief, peripapillary and macular data were obtained using the Optic Disc Cube 200 × 200 protocol and Macular Cube 512 × 128 protocol, respectively. Scans with signal strength < 7/10 or with artifact were excluded, in accordance with OSCAR-IB criteria.[17]

Peripapillary retinal nerve fiber layer (pRNFL) thicknesses were derived using the conventional Cirrus HD-OCT software, as described elsewhere.[16] A previously described segmentation algorithm was used for the generation of the thickness values for the rest of the retinal layers (macular ganglion cell layer/inner plexiform layer [GCIPL], inner nuclear layer [INL], and outer nuclear layer [ONL]).[18] In more detail, average thicknesses of the GCIPL, INL and ONL were calculated within an annulus, centered on the fovea, with an inner radius of 0.5 mm and an outer radius of 2.5 mm. Macular cube scans and segmentations were manually reviewed and scans with macular pathology or segmentation errors/failure were excluded. OCT results are reported in this manuscript in concordance with APOSTEL guidelines.[19]

Neuronally-enriched EVs (NEVs) isolation

The isolation of NEVs from the plasma of PwMS was performed by a well-described and extensively validated two-step protocol (first, particle precipitation to derive crude EVs, then, immunocapture targeting neuronal protein CD171, or L1 cell adhesion molecule [L1CAM].[20] Even though L1CAM is highly expressed in brain neuronal, it can also be found in other tissues (https://www.proteinatlas.org/ENSG00000198910-L1CAM/tissue) and certain tumors.[21] Nevertheless, it has been shown that plasma L1CAM+ EVs contain higher levels of neuronal-specific proteins compared to other plasma EVs, which suggests effective neuronal cargo enrichment.[20] Flow Cytometry analysis (optimized to reliably detect fluorescent EV signals) indicates that the immunoprecipitation targeting L1CAM results in a ~15.8-fold enrichment of immunoprecipitated L1CAM+ EVs compared to total plasma EVs (unpublished data).

NEV mitochondrial measures

Mitochondrial complex IV activity in NEVs was measured by the oxidation of reduced cytochrome c (ab109910; Abcam, Inc., Cambridge, MA), followed by ELISA (enzyme-linked immunoassay) for its quantity in the same samples. Complex V activity of NEVs was quantified for human complex V by the oxidative conversion of NADH to NAD+ (ab109714; Abcam, Inc., Cambridge, MA).

Statistical analysis

We removed outlier values greater than 3 standard deviations beyond the mean of each mitochondrial complex activity distribution (two mitochondrial complex IV values). For the longitudinal analysis, mitochondrial complex IV activity levels were log-transformed to approximate normal distribution. To simplify the interpretation of the results, the log-transformed mitochondrial complex IV activity levels and the mitochondrial complex V activity levels were then scaled.

We used partial Spearman’s correlation to test correlations between complex IV and V activity levels and brain volumetric measurements at baseline, adjusting for age.

The longitudinal analysis was performed utilizing mixed-effects models to assess the association of baseline mitochondrial complex activity and rates of brain substructure volume fraction and retinal layer thickness change. We modelled mitochondrial complex activity using linear terms, utilizing random subject-specific slopes and intercepts for the MRI measures and random eye-specific intercepts for the OCT measures. The models were adjusted for age at baseline, sex, and DMT category (injectables [interferons, glatiramer acetate] vs oral agents [dimethyl fumarate, diroximel fumarate, fingolimod, teriflunomide] vs infusions [ocrelizumab, natalizumab, rituximab] vs none) accounting for the duration of each DMT category utilizing a continuous time-varying variable. To ensure that adequate time has elapsed for the DMT to take effect and to account for the washout period after the discontinuation of each DMT, both the start and stop date in the model were pushed 6 months forward than the actual corresponding dates. OCT models were additionally adjusted for eye-specific history of ON.

All statistical analyses were performed using R Version 4.1.0 (https://www.r-project.org/). Statistical significance was defined as $p < 0.05$.

RESULTS

Cohort characteristics

Demographics and clinical characteristics of the cohort are presented in Table 1, along with mean mitochondrial complex IV and V activity levels. Participants were predominantly female (79%) with Relapsing Remitting MS (71%), had a mean age of 44.7 years, median disease duration of 12.5 years and median EDSS was 1.75. Median MRI and OCT follow-up durations were 3.4 and 4.9 years respectively. The median interval between the baseline blood draw and the first MRI and OCT scan was 81 and 7 days, respectively.

Complex IV activity levels are associated with baseline T2 lesion volume

We examined the relationship of complex IV and V activity levels with whole brain and brain substructure volumes at baseline. We noted a significant correlation between complex IV activity and T2 lesion volume (rho = 0.30, p = 0.046). We also noted a trend for an inverse correlation between complex IV activity and subcortical GM (rho = −0.29, p = 0.055) and cerebral WM (rho = −0.26, p = 0.083) though these did not reach statistical significance.

No significant correlations were noted between complex V activity levels and WBV, brain substructure volumes or T2 lesion volume.

Complex IV and V activity levels predict changes in brain volumetric and retinal thickness measures

Baseline mitochondrial complex IV and V activity levels were significantly associated with cortical gray matter (GM), subcortical GM, whole brain volume and GCIPL annualized rates of change, with higher mitochondrial complex IV (Figure 1A to E) and lower mitochondrial complex V (Figure 1F to J) activity predicting faster atrophy. Additionally, mitochondrial complex IV activity was significantly associated with the rate of pRNFL thinning.

The results are also shown in Table 2. Estimates and confidence intervals are expressed as a change in the annual rate of change of the outcome variable per unit (standard deviation) increase in the predictor variable.

DISCUSSION

In this study we found that levels of complex IV and complex V activity in NEVs from PwMS predicted future changes in brain and retinal layer volumetric measures, with higher complex IV activity and lower complex V activity being linked with faster whole brain, brain substructure and retinal atrophy.

Baseline complex IV activity predicted both whole brain, brain substructure, as well as retinal layer atrophy. During acute inflammation in active MS lesions, there is a diffuse mitochondrial injury, decreased complex IV activity and energy production.[1] As the lesions

and inflammation become chronic, demyelination and consecutive ion channel redistribution result in a state of increased energy demand in damaged neurons which results in a compensatory increase in mitochondrial number and activity.[22,23] Since complex IV activity is increased in chronically demyelinated axons,[2,3] its NEV levels may partly reflect the total amount of chronically demyelinated axons in the brain of PwMS. In this cohort we also noted a positive correlation between baseline T2 lesion volume and mitochondrial complex IV activity levels supporting this hypothesis. This provides a possible explanation for the observed relationship between higher baseline NEV mitochondrial complex IV activity level and greater subsequent brain and retinal atrophy.

Since complex V activity is critical for ATP production[24] and sustaining neuronal function and survival, it was not surprising that lower baseline levels of NEV mitochondrial complex V activity were associated with faster subsequent whole brain, substructure and retinal atrophy.

Mechanistically, we previously speculated in the setting of AD, that an imbalance with relative preservation of mitochondrial complex IV activity and diminution of mitochondrial complex V activity (as also seems to be the case with PwMS with greater degree of atrophy over time) may lead to increased availability of free electrons and production of reactive oxygen species, leading to increased neurodegeneration.[9] Inflammatory products of chronic inflammation can damage mitochondria and disrupt the respiratory chain function, which can lead in reactive oxygen species (ROS) production.[25] ROS-induced oxidative damage in mitochondria results in a vicious cycle of increasing ROS and decreasing ATP production.[26] Thus, increased levels of complex IV activity driven by the increased energy demand cause liberation of electrons and increased ROS production due to mitochondrial dysfunction. On the other hand, the lack of a proton gradient results in decreased complex V activity and reduced ATP production. The combined effects of increased ROS production and decreased ATP production would ultimately result in faster neurodegeneration as seen in our study.

Our study has certain limitations including the small sample size of the cohort, the retrospective nature of the study, lack of healthy control data and reference levels for NEV mitochondrial complex activity.

However, the results of this pilot study agree with current literature regarding the role of mitochondrial dysfunction in MS and suggest that circulating NEVs could be used to assess neuronal mitochondrial health in living people and as predictive biomarkers. Future large longitudinal studies of healthy controls and PwMS will be required to validate these findings, determine longitudinal changes in mitochondrial complex activity levels and establish the clinical utility of these EV measures in MS.

FUNDING

This study was supported in part by a grant from the Myelin Repair Foundation and EMD Serono Inc., USA, an affiliate of Merck KGaA, Darmstadt, Germany, through MS-LINK; and in part by the Intramural Research Program of the National Institute on Aging, NIH. PB is supported by a Harry Weaver Scholar Award from the National MS Society. The MRI equipment in this study was funded by NIH grant 1S10OD021648.

DECLARATION OF CONFLICTING INTERESTS

DCL, PJY, MV, JB, GK, KCF, DK declared no potential conflicts of interest.

ES has served on scientific advisory boards for Alexion, Viela Bio, Horizon Therapeutics and Genentech, received speaker honoraria from Alexion, Viela Bio and Biogen, and consulted for Ad Scientiam.

SS has received consulting fees from Medical Logix for the development of CME programs in neurology and has served on scientific advisory boards for Biogen, Genentech Corporation, TG therapeutics & Bristol Myers Squibb. He has received consulting fees from Carl Zeiss Meditec and Novartis. He is the PI of investigator-initiated studies funded by Genentech Corporation and Biogen. He has received equity compensation for consulting from JuneBrain LLC, a retinal imaging device developer.

PAC is PI on grants to JHU from Genentech and previously Principia. He has received consulting fees for serving as a scientific advisor from Biogen, Idorsia, Nervgen, Disarm (now Lilly), and Vaccitech.

PB is PI on grants to JHU from Genentech, Amylyx Pharmaceuticals, GSK and EMD-Serono.

REFERENCES

1. Mahad D, Ziabreva I, Lassmann H, et al. Mitochondrial defects in acute multiple sclerosis lesions. Brain 2008; 131: 1722–1735. [PubMed: 18515320]
2. Mahad DJ, Ziabreva I, Campbell G, et al. Mitochondrial changes within axons in multiple sclerosis. Brain 2009; 132: 1161–1174. [PubMed: 19293237]
3. Witte ME, Lars B, Rodenburg RJ, et al. Enhanced number and activity of mitochondria in multiple sclerosis lesions. The Journal of Pathology 2009; 219: 193–204. [PubMed: 19591199]
4. Rosenkranz SC, Shaposhnykov AA, Träger S, et al. Enhancing mitochondrial activity in neurons protects against neurodegeneration in a mouse model of multiple sclerosis. eLife 2021; 10: 1–60.
5. Licht-Mayer S, Campbell GR, Canizares M, et al. Enhanced axonal response of mitochondria to demyelination offers neuroprotection: implications for multiple sclerosis. Acta Neuropathologica 2020; 140: 143–167. [PubMed: 32572598]
6. D'Acunzo P, Pérez-González R, Kim Y, et al. Mitovesicles are a novel population of extracellular vesicles of mitochondrial origin altered in down syndrome. Science Advances 2021; 7: 5085–5097.
7. Yao PJ, Eren E, Petralia RS, et al. Mitochondrial Protrusions in Neuronal Cells. iScience 2020; 23: 101514. [PubMed: 32942173]
8. Kim KM, Meng Q, Perez de Acha O, et al. Mitochondrial RNA in Alzheimer's Disease Circulating Extracellular Vesicles. Front Cell Dev Biol 2020; 8: 581882. [PubMed: 33304899]
9. Yao PJ, Eren E, Goetzl EJ, et al. Mitochondrial Electron Transport Chain Protein Abnormalities Detected in Plasma Extracellular Vesicles in Alzheimer's Disease. Biomedicines 2021; 9: 1587. [PubMed: 34829816]
10. Goetzl EJ, Wolkowitz OM, Srihari VH, et al. Abnormal levels of mitochondrial proteins in plasma neuronal extracellular vesicles in major depressive disorder. Mol Psychiatry 2021; 26: 7355–7362. [PubMed: 34471251]
11. Bhargava P, Nogueras-Ortiz C, Kim S, et al. Synaptic and complement markers in extracellular vesicles in multiple sclerosis. Multiple Sclerosis Journal 2021; 27: 509–518. [PubMed: 32669030]
12. Bhargava P, Nogueras-Ortiz C, Chawla S, et al. Altered Levels of Toll-Like Receptors in Circulating Extracellular Vesicles in Multiple Sclerosis. Cells 2019; 8: 1058.
13. Dewey BE, Zhao C, Reinhold JC, et al. DeepHarmony: A deep learning approach to contrast harmonization across scanner changes. Magnetic Resonance Imaging 2019; 64: 160–170. [PubMed: 31301354]
14. Huo Y, Plassard AJ, Carass A, et al. Consistent Cortical Reconstruction and Multi-atlas Brain Segmentation. NeuroImage 2016; 138: 197. [PubMed: 27184203]
15. Beer JC, Tustison NJ, Cook PA, et al. Longitudinal ComBat: A method for harmonizing longitudinal multi-scanner imaging data. NeuroImage 2020; 220: 117129. [PubMed: 32640273]
16. Syc SB, Warner CV., Hiremath GS, et al. Reproducibility of high-resolution optical coherence tomography in multiple sclerosis. Multiple sclerosis (Houndmills, Basingstoke, England) 2010; 16: 829–839.

17. Schippling S, Balk LJ, Costello F, et al. Quality control for retinal OCT in multiple sclerosis: validation of the OSCAR-IB criteria. Multiple sclerosis (Houndmills, Basingstoke, England) 2015; 21: 163–170.

18. Lang A, Carass A, Hauser M, et al. Retinal layer segmentation of macular OCT images using boundary classification. Biomedical Optics Express 2013; 4: 1133. [PubMed: 23847738]

19. Aytulun A, Cruz-Herranz A, Aktas O, et al. APOSTEL 2.0 Recommendations for Reporting Quantitative Optical Coherence Tomography Studies. Neurology 2021; 97: 68–79. [PubMed: 33910937]

20. Mustapic M, Eitan E, Werner JK, et al. Plasma extracellular vesicles enriched for neuronal origin: A potential window into brain pathologic processes. Frontiers in Neuroscience 2017; 11: 278. [PubMed: 28588440]

21. Altevogt P, Doberstein K, Fogel M. L1CAM in human cancer. International Journal of Cancer 2016; 138: 1565–1576. [PubMed: 26111503]

22. Ohno N, Chiang H, Mahad DJ, et al. Mitochondrial immobilization mediated by syntaphilin facilitates survival of demyelinated axons. Proceedings of the National Academy of Sciences 2014; 111: 9953–9958.

23. Barcelos IP de, Troxell RM, Graves JS. Mitochondrial Dysfunction and Multiple Sclerosis. Biology 2019; 8: 37.

24. DiMauro S, Schon EA. Mitochondrial Respiratory-Chain Diseases. N Engl J Med 2003; 348: 2656–2668. [PubMed: 12826641]

25. Murphy MP. How mitochondria produce reactive oxygen species. Biochemical Journal 2009; 417: 1–13. [PubMed: 19061483]

26. Mahad DH, Trapp BD, Lassmann H. Pathological mechanisms in progressive multiple sclerosis. The Lancet Neurology 2015; 14: 183–193. [PubMed: 25772897]

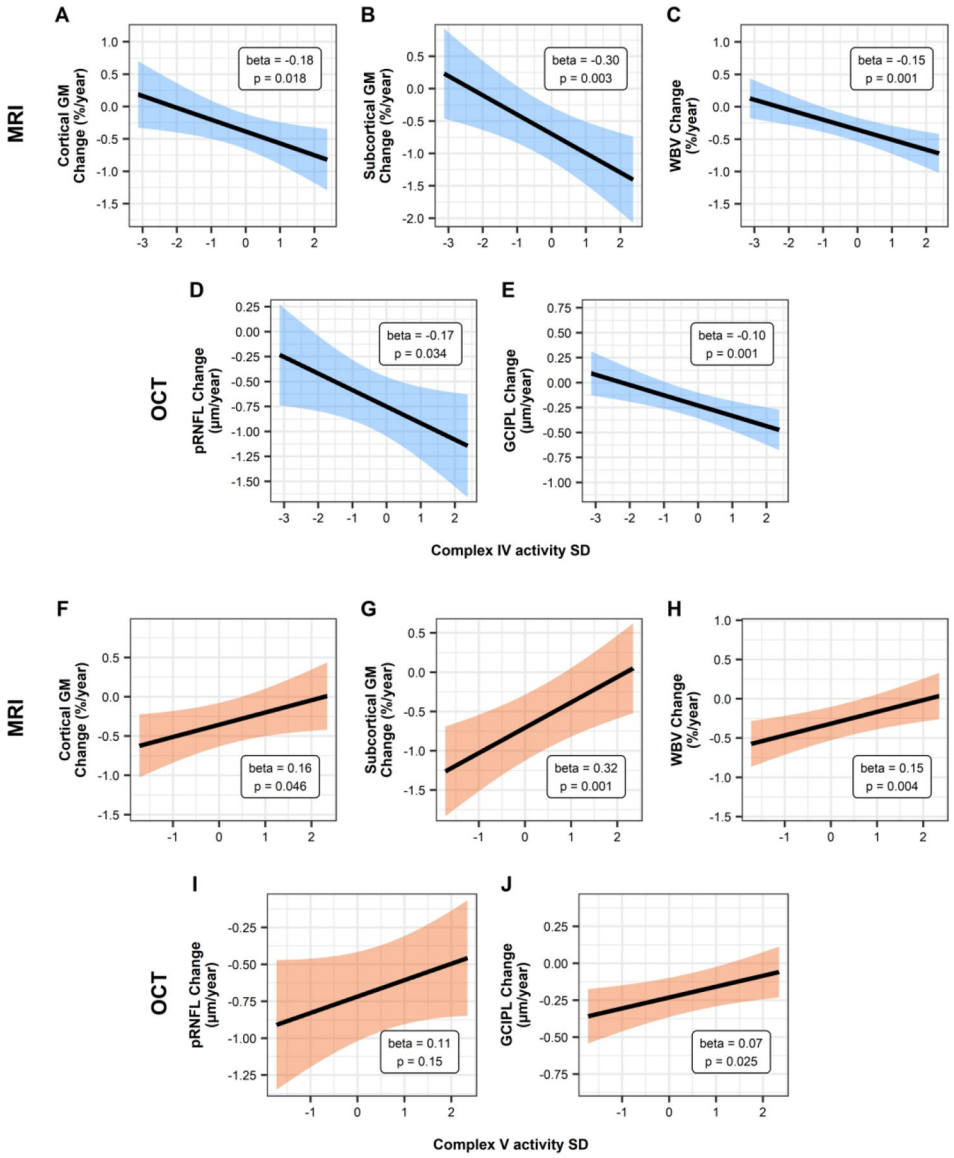

Figure 1. Association between baseline mitochondrial complex IV and V activities and MRI and OCT derived measures.

Relationship of the estimated annualized rates of change for MRI (WBV and brain substructures) and OCT (pRNFL and GCIPL) measures with scaled baseline complex IV (Panels A-E) and complex V (Panels F-J) activity using linear mixed-effects models. Shaded area denotes the 95% confidence interval. MRI models are adjusted for age at baseline, sex, and DMT-class, while OCT models are additionally adjusted for history of optic neuritis. GCIPL = macular ganglion cell layer/inner plexiform layer, GM = gray matter, MRI = magnetic resonance tomography, OCT = optical coherence tomography, pRNFL = peripapillary retinal nerve fiber layer, SD = standard deviation, WBV = whole brain volume

Table 1.

Demographics and Clinical Characteristics

Subjects[a] (eyes)	48 (90)
Age, years, mean (SD)	44.7 (11.6)
Female, n (%)	38 (79%)
Race, n (%)	
White	43 (90%)
African American	2 (4%)
Other	3 (6%)
EDSS, median (IQR)	1.75 (0 – 3.0)
Symptom duration, years, median (IQR)	12.5 (7.8 – 18.5)
Disease Subtype, n (%)	
Relapsing-remitting	34 (71%)
Secondary progressive	12 (25%)
Primary progressive	2 (4%)
Disease Modifying Therapy at Baseline, n (%)	
Infusion	3 (6%)
Oral	1 (2%)
Injectable	15 (31%)
None	29 (61%)
Eyes with history of ON, n (%)	34 (38%)
Baseline NEV Complex IV activity, mOD/min, mean (SD)	1.07×10^{-4} (0.4×10^{-4})
Baseline NEV Complex V activity, mOD/min, mean (SD)	0.0379 (6×10^{-4})
MRI follow-up time, years, median (IQR)	3.4 (2.1 – 4.3)
OCT follow-up time, years, median (IQR)	4.9 (4.1 – 6.3)

[a]One participant did not have OCT follow-up

EDSS = Expanded Disability Status Scale, IQR: interquartile range, MRI: magnetic resonance imaging, NEV: extracellular vesicles enriched for neuronal origin, OCT: optical coherence tomography, ON: Optic neuritis, SD = standard deviation

Table 2.

Baseline Complex IV and V activity levels as predictors of imaging outcomes

		Baseline Complex IV activity		Baseline Complex V activity	
		Estimate[a] (95% CI)	**p-value**	**Estimate[a] (95% CI)**	**p-value**
MRI measures[d] (%/year)	Cortical GM	−0.18 (−0.33 to −0.03)	**0.018** [b]	0.16 (0.003 to 0.31)	**0.046** [b]
	Cerebral WM	−0.15 (−0.36 to 0.06)	0.16[b]	0.21 (−0.01 to 0.44)	0.056[b]
	Subcortical GM	−0.30 (−0.50 to −0.10)	**0.003** [b]	0.32 (0.13 to 0.52)	**0.001** [b]
	Thalamus	−0.14 (−0.41 to 0.12)	0.29[b]	0.33 (0.09 to 0.57)	**0.008** [b]
	Caudate nucleus	−0.51 (−0.74 to −0.28)	**<0.001** [b]	0.35 (0.13 to 0.58)	**0.002** [b]
	Putamen	−0.42 (−0.65 to −0.20)	**<0.001** [b]	0.25 (0.01 to 0.49)	**0.043** [b]
	Globus pallidus	−0.66 (−1.07 to −0.25)	**0.002** [b]	0.48 (0.05 to 0.91)	**0.028** [b]
	WBV	−0.15 (−0.24 to −0.07)	**0.001** [b]	0.15 (0.05 to 0.25)	**0.004** [b]
	T2 lesion	1.32 (−2.32 to 4.96)	0.47[b]	−0.17 (−3.60 to 3.27)	0.92[b]
OCT measures (μm/year)	pRNFL	−0.17 (−0.32 to −0.01)	**0.034** [c]	0.11 (−0.04 to 0.25)	0.15[c]
	GCIPL	−0.10 (−0.16 to −0.04)	**0.001** [c]	0.07 (0.01 to 0.13)	**0.025** [c]
	INL	−0.03 (−0.07 to 0.004)	0.079[c]	0.05 (0.01 to 0.09)	**0.006** [c]
	ONL	−0.07 (−0.13 to 0.001)	0.054[c]	0.12 (0.05 to 0.18)	**<0.001** [c]

[a]Parameter estimates for baseline complex IV and V activity by time interaction and 95% confidence intervals are given for each model. The estimate value reflects the effect of 1 standard deviation increase in baseline complexes activity

[b]P-values derived from linear mixed-effects models adjusted for age at baseline, sex, and DMT-class; statistically significant values (<0.05) are bolded

[c]P-values derived from linear mixed-effects models adjusted for age at baseline, sex, DMT-class and history of optic neuritis; statistically significant values (<0.05) are bolded

[d]Brain substructures are normalized to the median intracranial volume for each participant

CI = confidence intervals, GCIPL = macular ganglion cell layer/inner plexiform layer, GM = gray matter, INL = inner nuclear layer and outer plexiform layers, MRI = magnetic resonance imaging, OCT = optical coherence tomography, ONL = outer nuclear layer including the photoreceptor segments, pRNFL = peripapillary retinal nerve fiber layer, WBV = whole brain volume, WM = white matter